CHEMISTRY
AN ASIAN JOURNAL
ACES
FULL PAPER

DOI: 10.1002/asia.201402576

Fluorocarbon and Hydrocarbon N-Heterocyclic (C5–C7) Imidazole-Based Liquid Crystals

Hongren Chen,[a] Fengying Hong,[a] Guang Shao,[c] Deyu Hang,[d] Lei Zhao,[d] and Zhuo Zeng*[a, b]

Abstract: By using three synthetic protocols, a series of fluorocarbon and hydrocarbon N-heterocyclic imidazole-based liquid crystals (LCs) and related imidazolium-based ionic liquid crystals (ILCs) have been prepared. The ring size of the N-heterocycle and the length of the N-terminal chain (on the imidazolium unit in the ILCs) were modified, and the influence of these structural parameters on liquid-crystal phases was investigated by means of polarizing optical microscopy (POM), differential scanning calorimetry (DSC), and X-ray diffraction (XRD). These new ILCs exhibit a disordered smectic phase (SmA), good thermal stabilities, a broad smectic phase range, a high dipole moment, relatively low melting points, but high clearing points and strong emission fluorescence relative to imidazole-based LCs. These encouraging results have led us to believe these fluorocarbon and hydrocarbon N-heterocyclic imidazole-based LCs and related imidazolium-based ILCs could be used as new liquid-crystalline materials.

Keywords: fluorine · heterocycles · ionic liquids · mesophases · phase transitions

Introduction

Liquid crystals (LCs) as soft materials have attracted considerable attention owing to their fascinating properties[1] and their successful applications in commerce.[2] Ionic liquid crystals are a class of liquid-crystalline compounds that contain salts of cations and their counterpart anions. They can be considered materials that possess the properties of both liquid crystals and ionic liquids. They are significantly different from conventional neutral LCs but still display mesophases. Their useful properties include ion conductivity, nonvolatility, low viscosity, low melting points, and tunable polarity.[3]

ILCs with different cations have been described in the literature, such as ammonium, phosphonium, pyridinium, and so forth.[4] Imidazolium salts have been intensively investigated as ionic liquids and also introduced into ILC systems.[5–10] This is because the imidazolium unit is an excellent platform that can be designed to promote liquid-crystalline phases and is easily doped by a large diversity of anions.[11] Imidazolium-based ILCs including symmetrical and unsymmetrical molecular frameworks have been generated and most of them show smectic phases.[12] Recently, mesomorphic imidazolium salts were also used as new vectors for small interfering RNA (siRNA) transfection.[13]

Most of the organic compounds known for optoelectronic applications still have some major limitations such as low electron conductivity or luminescence efficiency. An alternative method to bypass these limitations is to introduce an electron-acceptor group such as oxadiazole,[14] quinoline,[15] or other heterocycle moieties.[16] The introduction of a polar ring into the liquid-crystalline core is a promising approach to the design of novel liquid crystals for applications in advanced functional materials. Structures such as N-heterocycles should prove to be highly valuable for further investigation because of their large dielectric constant, great electron-transport abilities, and strong electron-withdrawing properties.[17] The coupling of N-heterocycles and imidazole in an ionic compound would, in principle, enhance both its electron transport and conductivity to bypass those limitations. Introducing a fluorine atom or fluorinated group into liquid-crystal systems will remarkably modify their melting points, mesophase morphologies, transition temperatures, and many other very important physical properties, such as dielectric anisotropy, optical anisotropy, and viscoelastic properties. Many fluorinated LCs display excellent modified

[a] H. Chen, F. Hong, Prof. Z. Zeng
College of Chemistry and Environment
South China Normal University
Guangzhou, 510006 (China)
Fax: (+0086) 2039310287
E-mail: zhuoz@scnu.edu.cn

[b] Prof. Z. Zeng
Key Laboratory of Organofluorine Chemistry
Shanghai Institute of Organic Chemistry
Chinese Academy of Sciences
Shanghai, 200032 (China)

[c] Dr. G. Shao
School of Chemistry and Chemical Engineering
Sun Yat-sen University
Guangzhou, 510275 (China)

[d] Dr. D. Hang, L. Zhao
Beijing Bayi Space LCD Materials Technology Co., Ltd.
Beijing 102205 (China)

Supporting information for this article is available on the WWW under http://dx.doi.org/10.1002/asia.201402576.

properties, and investigations on fluorinated ILCs have reported prospective applications owing to the existence of fluoro substituents.[18] There is interest in the development of some fluorinated imidazole-based LCs and related imidazolium-based ILCs derivatives in an effort to establish their structure–property relationships, and to target potential liquid-crystal display applications.[13]

In this work, we report the design and syntheses of fluorocarbon and hydrocarbon imidazole-based liquid crystals (LCs) and their related imidazolium-based ionic liquid crystals (ILCs). The impact on their properties of N-heterocycles in varying sizes, alkyl chain lengths, and anions has been investigated. The coupling of a fluorinated heterocycle and imidazole moiety in these new compounds should exhibit some interesting electron-transport properties because of their ability to impart lateral and/or longitudinal dipoles in addition to the accompanying changes in their molecular geometry.[19] Their mesomorphic properties, some of their physicochemical properties such as UV and fluorescence, and their thermal stability properties were investigated.

Results and Discussion

Synthesis

Three synthetic protocols for the preparation of N-heterocyclic imidazole-based compounds (**M2F**, **M5F**–**M7F**, **M5H**–**M7H**) have been employed in this article. The first synthetic routine was as follows: a) As we described in our previous experiments,[20] a series of trifluoromethanesulfonic acid polyfluoroalkyldiyl **1f** and **2f** and 4-toluene sulfonyl alkyldiyl (**1h**–**3h**) esters were treated with 4-iodobenzenamine in the presence of Et_3N and CH_3CH_2OH to give fluorocarbon and hydrocarbon N-heterocyclic (C5–C7) iodobenzene compounds **I5H**–**I7H**, **I5F**, and **I6F** (Scheme 1). Dehydrofluorination of **I5F** with an excess amount of *t*BuONa in DMSO at 90 °C for 12 h generated the 3,4-difluoro-1-(4-iodophenyl)pyrrole (**I2F**) in high yields. When **I6F** was treated with an excess amount of *t*BuONa in DMSO under a range of temperatures (50–150 °C), a mixture of compounds was observed by TLC that could not be separated by normal column chromatography owing to their similar polarities (Scheme 2). b) Transition-metal-catalyzed Ullmann-type coupling is one of the most important methods in the formation of imidazole compounds.[21] Among the transition-metal catalysts tested, the copper-catalyzed reaction was clearly the best choice. Two different bases (NaOH,[22] K_3PO_4[23]) were chosen to compare their yields (Scheme 3). We found that using K_3PO_4 as base gave better results in terms of yield in dimethylformamide (DMF) relative to NaOH in DMSO under ligand-free conditions (Table 1). However, fluorinated N-heterocyclic compound **I5F** was dehydrofluorinated to yield **M2F**, and **I6F** gave an inseparable mixture under these alkaline Ullmann-type coupling conditions.

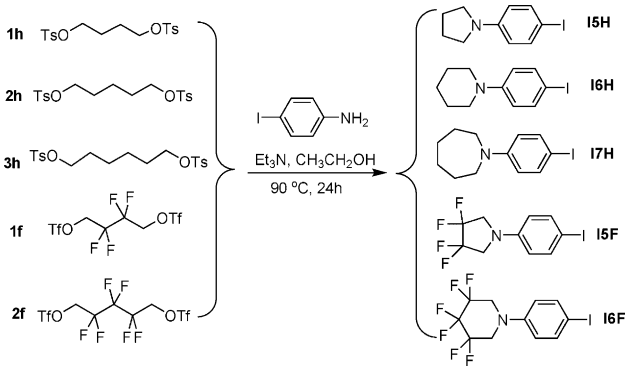

Scheme 1. Synthesis of fluorocarbon and hydrocarbon N-heterocyclic (C5–C7) iodobenzene.

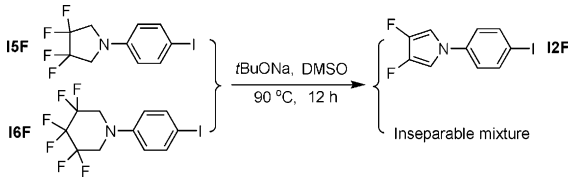

Scheme 2. Dehydrofluorination of compound **I5F** and **I6F**.

Using the second synthetic routine, 4-(1*H*-imidazol-1-yl)aniline was prepared first, then further treated with trifluoromethanesulfonic acid polyfluoroalkyldiyl and 4-toluene sulfonyl alkyldiyl esters, **1f** and **1h**, to produce N-heterocyclic

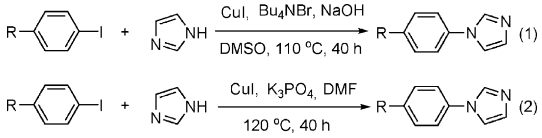

Scheme 3. Ullmann-type coupling reaction in different conditions.

Abstract in Chinese:

本文合成了一系列新型的含氟及无氟氮杂环咪唑液晶。这些化合物的 POM, DSC, XRD, TG 和荧光测试表明，化合物的液晶性能受末端（C5-C7）氮杂环及咪唑上烷基链的影响。末端为 3,3,4,4-四氟吡咯烷的化合物 M5F 为扭曲的 N1-信封式结构呈现扇形的近晶 A 相，而无氟氮杂环咪唑化合物 M5-7H 呈现马赛克的近晶 E 相。通过比较中性咪唑液晶分子和其离子盐衍生物，发现后者呈现近晶 A 相，有更好的热稳定性，更宽的液晶相，大的偶极距，相对低的熔点和高的清亮点及强的荧光。这些含氟和无氟氮杂环咪唑及咪唑盐化合物可作为潜在的新型液晶材料。

Table 1. Prepared N-heterocyclic imidazoles by Ullmann-type coupling reaction.

R	Products	Yield 1 [%]	Yield 2 [%]
	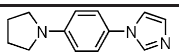 **M5H**	55.9	90.2
	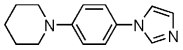 **M6H**	56.5	91.3
	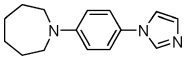 **M7H**	55.8	89.3
	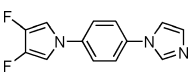 **M2F**	42.3	26.3
	**M6F** (inseparable mixture)	0	0
	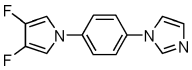 **M2F**	58.4	92.5
NH_2	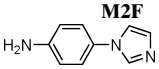 **MNH_2**	57.1	89.5

imidazolium compounds. However, their yields were very poor (**M5H** 5.2%, **M5F** 1.9%) (Scheme 4). It is possible that it is easy to treat imidazole with **1f**[24] and **1h**[25] to give the corresponding quaternary imidazolium compounds.

Syntheses of fluorinated N-heterocyclic imidazole-based LCs by using an alkaline Ullmann-type coupling reaction and cyclization of 4-(1*H*-imidazol-1-yl)aniline were not successful, since fluorine was easily eliminated in the course of the Ullmann-type coupling reaction and 4-(1*H*-imidazol-1-yl)aniline was quaternized with **1f** and **1h** under the cyclization reaction.

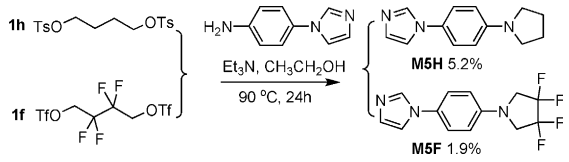

Scheme 4. Cyclization of 4-(1*H*-imidazol-1-yl)aniline.

Therefore, the third synthetic routine was adopted. Fluorinated N-heterocyclic imidazoles **M5F**–**M7F** were prepared by Debus–Radziszewski imidazole synthesis[26] in a reasonably good yield. It is worth noting that these protocols are generally operated in volatile compounds with a base. Fluorocarbon N-heterocyclic anilines (**N5F**–**N7F**) were obtained by reactions of trifluoromethanesulfonic acid polyfluoroalkyldiyl **1f**–**3f** with two equivalents of *p*-phenylenediamine in the presence of Et_3N in high yields. N-Heterocyclic imidazoles were obtained in a three-step procedure as described in Debus–Radziszewski imidazole synthesis. The N-heterocyclic anilines were treated with glyoxal through the nucleophilic addition to form imine compounds, then they were treated with formaldehyde and ammonium chloride to yield quaternary ammonium salt. The quaternary ammonium salt was further treated with phosphoric acid in methanol to give the target compounds, fluorocarbon N-heterocyclic imidazoles (**M5F**–**M7F**), in high yield (Scheme 5). These N-heterocyclic imidazole compounds (**M2F**, **M5F**–**M7F**, **M5H**–**M7H**) were quaternized with the appropriate 1-bromotetradecane or 1-bromohexadecane bromides in acetonitrile to yield the N-heterocyclic imidazolium-based ILCs in high yields (**2F-14/18,** (**5**–**7**)**F-14/18,** (**5**–**7**)**H-14/18**). The bromine ions of representative compounds **5F-14** and **5F-18** were exchanged with $NaBF_4$ in acetone to give **5F-14B** and **5F-18B** (Scheme 6).

Liquid-Crystalline Properties

The phase transitions and thermodynamic data of the nonionic imidazoles (**M5F**–**M7F/H**, **M2F**) and the corresponding imidazolium salts ((**5**–**7**)**H-14/18**, (**5**–**7**)**F-14/18**, **2F-14/18**, **5F-14/18B**) were investigated by means of differential scanning calorimetry (DSC), polarizing optical microscopy (POM), thermogravimetric analysis (TGA), and for selected compounds, variable-temperature X-ray diffraction (VTXRD).

The transition temperatures of the nonionic imidazoles **M5F/H**–**M7F/H** and **M2F** are collected in Table 2. All hydrocarbon N-heterocyclic nonionic imidazole compounds exhibit a thermotropic mesomorphic phase. A mosaic texture of crystal smectic E (SmE) phase was observed by means of POM for pyrrolidine-, piperidine-, and azepane-based imidazole compounds **M5H**–**M7H** (Figure 1a–c). They exhibited a narrow phase (e.g., **M5H** (Cr 178.9 °C, SmE

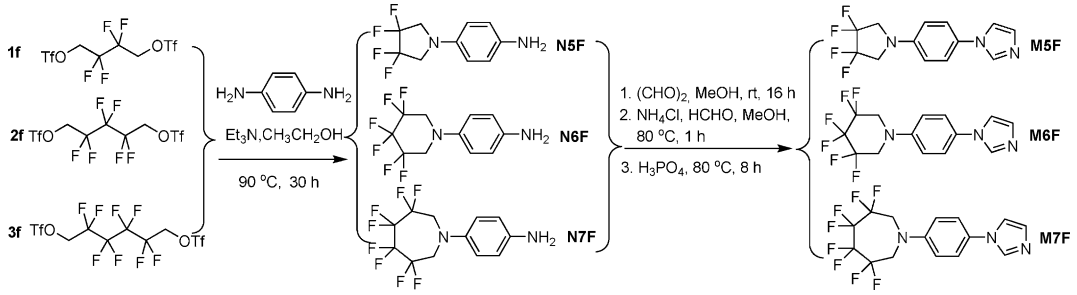

Scheme 5. Synthesis of N-heterocyclic imidazole LCs by means of the Debus–Radziszewski procedure.

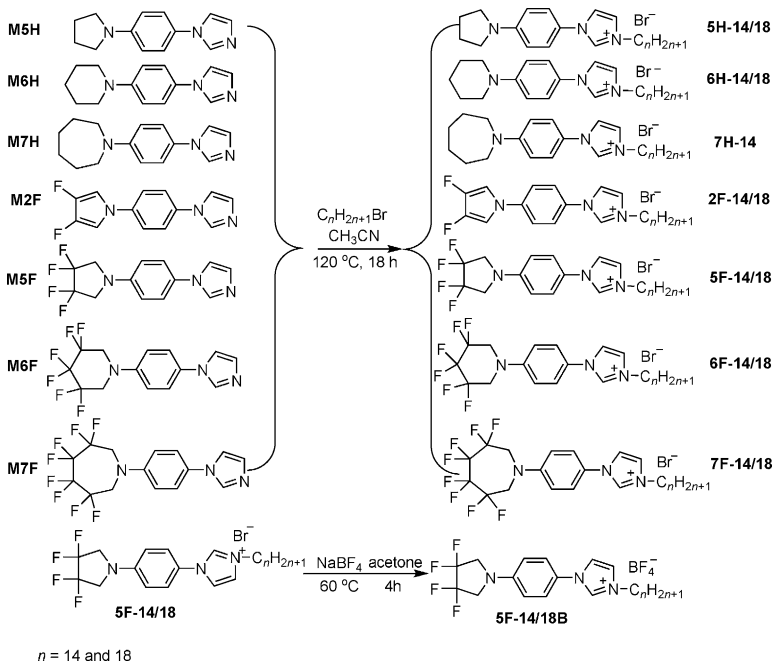

Scheme 6. Synthesis of N-heterocyclic imidazolium-based ILCs.

Table 2. Thermal behavior of the N-heterocyclic imidazole-based LCs.

Compound	Transition temperatures [°C][a]	Enthalpies of transition [J g^{-1}]	
M2F	Cr 179.9 [2.56]	SmE 185.5[b]	iso
M5F	Cr 175.4 [3.94]	SmE 178.0[b]	iso
M6F	Cr 82.1 [8.30]		iso
M7F	Cr 115.7 [4.73]		iso
M5H	Cr 178.9 [3.03]	SmE 187.9[b]	iso
M6H	Cr 104.2 [13.98]	SmE 118.7[b]	iso
M7H	Cr 68.5 [6.47]	SmE 73.8[b]	iso

[a] Transition temperature and enthalpy change (in square brackets) were determined by DSC (peak temperature, first heating scan, 5 K min^{-1-1}) and confirmed by POM. Cr = crystalline solid, SmE = crystal smectic E, iso = isotropic liquid state. [b] Transition temperatures were determined by POM.

187.9 °C; Cr = crystalline solid), **M6H** (Cr 104.2 °C, SmE 118.7 °C), **M7H** (Cr 68.5 °C, SmE 73.8 °C); Table 2). However, for fluorocarbon N-heterocyclic imidazole compounds, only 3,3,4,4-tetrafluoropyrrolidine- and 3,4-difluoropyrrole-based imidazole compounds **M2F** and **M5F** show a thermotropic mesomorphic phase. Compound **M5F** with 3,3,4,4-tetrafluoropyrrolidine as the terminal group also displayed a mosaic texture of the crystal smectic E phase (Figure 1d), whereas **M6F** and **M7F** melted into an isotropic liquid at 82.1 and 115.7 °C directly with no liquid-crystal texture being observed. Upon increasing the terminal N-heterocycle size from pyrrolidine to azepane, their melting points decrease dramatically, (e.g., **M5H**: m.p. 178.9 °C **M6H**: m.p. 104.2 °C **M7H**: m.p. 68.5 °C). When comparing fluorocarbon N-heterocyclic imidazole with hydrocarbon N-heterocyclic imidazole, **M6F** with 3,3,4,4,5,5-hexafluoropiperidine as its terminal group shows the lowest melting point, 82.1 °C.

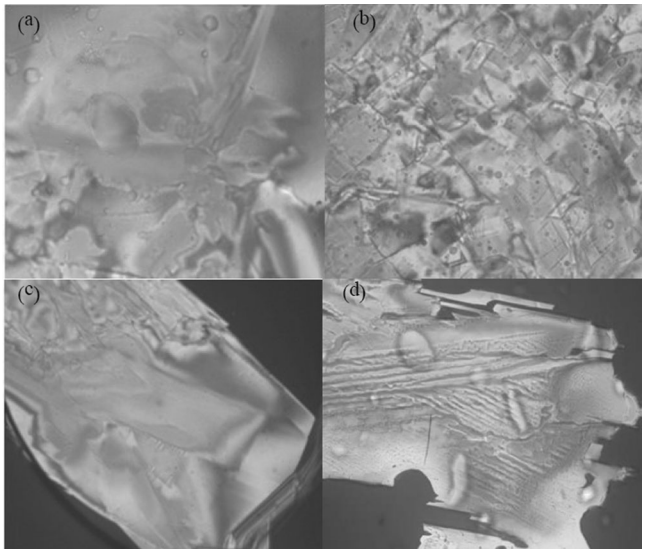

Figure 1. a) Mosaic texture of SmE upon cooling to 179 °C for **M5H**. b) Mosaic texture of SmE upon cooling to 105 °C for **M6H**. c) Mosaic texture of SmE upon cooling to 70 °C for **M7H**. d) Mosaic texture of SmE upon cooling to 172 °C for **M5F**.

In the series of the imidazolium salts (**5**–**7**)**H-14/18**, (**5**–**7**)**F-14/18**, **2F-14/18**, and **5F-14/18B**, all compounds show a thermotropic liquid-crystalline phase, with the exception of the terminal hydrocarbon seven-membered ring N-heterocyclic compounds **7H-14** (Table 3).

Imidazolium bromides with terminal fluorocarbon and hydrocarbon N-heterocycles, (**5**–**7**)**F-14/18** and **2F-14/18**, have a broader range of mesomorphic phases than the series of nonionic imidazoles **M5**–**7F/H** and **M2F**. These compounds displayed disordered SmA mesophases (e.g., Figure 2). Some of these compounds have a very wide smectic range; for example, **2F-18** has a smectic phase range of 113.6 °C. As can be seen from Table 3, as the terminal N-heterocycle size increases from a five- to a seven-membered ring, the range of hydrocarbon N-heterocyclic compounds narrows rapidly (e.g., **5H-14** (Cr 100.8 °C SmA 123.9 °C), **6H-14** (Cr 64.1 °C SmA 69.6 °C); see Table 3), and **7H-14** is an isotropic liquid at 36.8 °C directly with no liquid-crystal texture being observed, whereas the range of fluorocarbon N-heterocyclic compounds first decreases and then increases upon increasing the terminal N-heterocycle size (e.g., **5F-14** (Cr 89.1 °C

Table 3. Thermal behavior of the N-heterocyclic imidazolium-based ILCs.

Compound	Transition temperatures [°C][a]	Enthalpies of transition [J g^{-1}]		*Td* [°C][b]
5F-14	Cr 89.1 [2.29]	SmA 157.2 [4.28]	iso	259
5H-14	Cr 100.8 [4.78]	SmA 123.9 [4.20]	iso	257
2F-14	Cr 135.7 [1.10]	SmA 206.9 [0.89]	iso	255
6F-14	Cr 106.0 [12.21]	SmA 112.3[c]	iso	267
6H-14	Cr 64.1 [19.16]	SmA 69.6[c]	iso	259
7F-14	Cr 145.7 [2.04] Cr′ 148.7 [2.95]	SmA 180.4 [8.76]	iso	264
7H-14	Cr 36.8 [10.20]		iso	261
5F-18	Cr 108.3 [2.94]	SmA 165.3 [0.23]	iso	247
5H-18	Cr 106.0 [3.67] Cr′ 111.7 [1.44]	SmA 121.5 [1.21]	iso	263
2F-18	Cr 122.8 [7.28] Cr′ 135.3 [3.68]	SmA 248.9 [1.91]	iso	250
6F-18	Cr 107.5 [9.06]	SmA 116.2[c]	iso	263
6H-18	Cr 61.2 [19.82]	SmA 71.8[c]	iso	266
7F-18	Cr 80.2 [8.07]	SmA 182.3 [18.32]	iso	262
5F-14B	Cr 84.1 [14.42]	SmA 251.5[c]	iso	273
5F-18B	Cr 63.7 [8.26] Cr′ 83.6 [4.48]	SmA 254.1[2.56]	iso	268

[a] Transition temperature and enthalpy change (in square brackets) were determined by DSC (peak temperature, first heating scan, 5 K min^{-1-1}) and confirmed by POM. Cr = crystalline solid, N = nematic phase, SmA = Smectic A, iso = isotropic liquid state. [b] Transition temperatures were determined by POM. [c] Decomposition temperature.

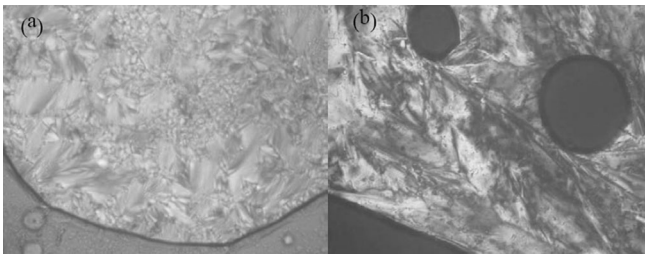

Figure 2. a) Texture of the SmA upon cooling to 166 °C for **2F-14**. b) Texture of the SmA upon cooling to 177 °C for **7F-14**.

SmA 157.2 °C), **6F-14** (Cr 106.0 °C SmA 112.3 °C), **7F-14**, (Cr′ 148.7, SmA 180.4 °C); see Figure 3). In contrast to when the N-heterocycle is the same size as the terminal group, the smectic A phase of terminal fluorocarbon N-heterocyclic compounds is broader than that of terminal hydrocarbon N-heterocyclic compounds (e.g., **5F-18** (Cr 108.3 °C SmA 165.3 °C), **5H-18** (Cr′ 111.7, SmA 121.5), **6F-18** (Cr 107.5 °C SmA 116.2 °C), **6H-18** (Cr 61.2, SmA 71.8)).

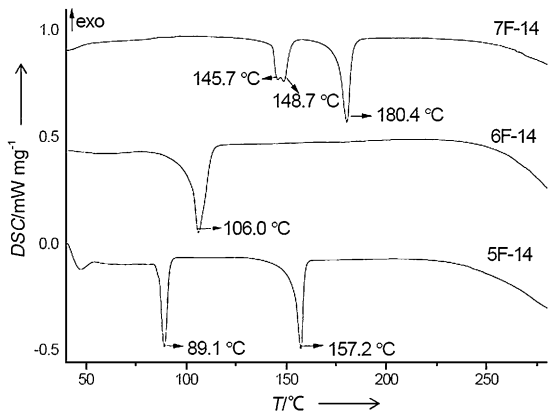

Figure 3. DSC heating curves of compounds **5F-14**, **6F-14**, and **7F-14**.

In general, the introduction of terminal nonfluorinated pyrrolidine, piperidine, and azepane causes a decrease in the melting temperature relative to the introduction of 3,4- difluoropyrrole, 3,3,4,4-tetrafluoropyrrolidine, 3,3,4,4,5,5-hexafluoropiperidine, and 3,3,4,4,5,5,6,6-octafluoroazepane compounds, for example, **5F-18** (m.p. 108.3 °C), **5H-18** (m.p. 106.0 °C), **6F-18** (m.p. 107.5 °C), **6H-18** (m.p. 61.2 °C), whereas compound **5F-14** has a lower melting point (89.1 °C) than compound **5H-14**. In addition, upon increasing the terminal N-heterocycle size from pyrrolidine to azepane, their melting points decrease dramatically (e.g., **5H-14** (m.p. 100.8 °C), **6H-14** (m.p. 64.1 °C), **7H-14** (m.p. 36.8 °C)). However, the melting points of the terminal fluorocarbon N-heterocycle are different when the substituent is $nC_{14}H_{29}$, such as in (**5**–**7**)**F-14**, for which the melting points decrease with expansion of the terminal N-heterocycle size from 3,3,4,4-tetrafluoropyrrolidine to 3,3,4,4,5,5,6,6-octafluoroazepan. The melting points increase upon increasing the terminal fluorocarbon N-heterocycle size when the substituent is $nC_{18}H_{37}$ as in (**5**–**7**)**F-18**. It shows that the length of the N-terminal chain (on the imidazolium unit in the ILCs) influences the melting points of terminal fluorocarbon N-heterocyclic imidazolium-based ILCs.

The 3,4-difluoropyrrole-based ionic liquid crystals with Br^- anion, **2F-14**/**18**, have the highest clearing point relative to the other terminal fluorocarbon and hydrocarbon N-heterocyclic compounds (e.g., **2F-14** and **2F-18** at c.p. 206.9 and 248.9 °C respectively, and **5F-14**, **5H-14**, and **7F-14** at c.p. 157.2, 123.9, and 180.4 °C).

The anion also plays a crucial role in determining the melting point and smectic phase range. The salts with BF_4^- anion have lower melting points lower and a much broader smectic phase range than the corresponding salts with Br^- anion (e.g., **5F-18** (Cr 108.3 °C SmA 165.3 °C), **5F-18B** (Cr′ 84.1 °C SmA 254.1 °C)).

X-ray Diffraction

Smectic phases were observed for these compounds by means of POM. To obtain further information on the molecular arrangements in the mesophase, variable-temperature X-ray diffraction (VT-XRD) experiments were performed on **M5H** and **2F-14** (for **5F-14**, **6F-14**, **7F-14**, and **5F-18B**; see the Supporting Information). The diffraction patterns obtained for compounds **M5H** and **2F-14** are shown in Figures 4 and 5, respectively.

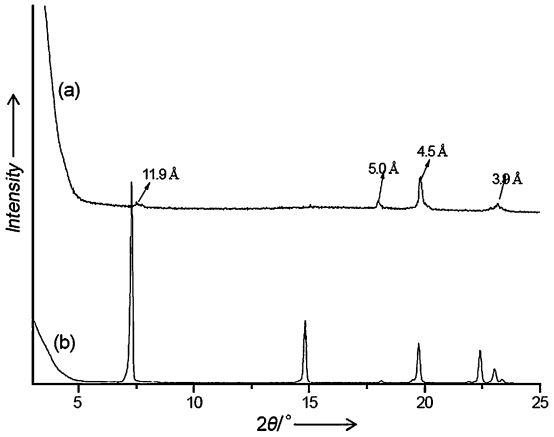

Figure 4. X-ray diffraction pattern of compound **M5H** at a) 184 and b) 50 °C (before heating).

Figure 4 shows the diffraction diagram of the phase transitions of **M5H** taken at 184 and 50 °C. When the measuring temperature was cooled to 184 °C only one sharp reflection at 7.52° was seen with corresponding *d* spacings of 11.9 Å in the small-angle region. Three sharp reflections were seen with *d* spacings of 5.0, 4.5, and 3.9 Å in the wide-angle region (Figure 4a). The liquid-crystal state for SmE, SmG, and SmI shows several sharp outer diffraction peaks as previously reported.[27] The optical polarizing micrograph (Figure 1a) reveals a mosaic texture of SmE for **M5H** in this temperature range. Both results are consistent with a crystal smectic E structure, and this is consistent with the fact that a 1-methylimidazolium (MIm) group attached to rod-shaped LCs has commonly yielded SmA and SmE phases.[28] When the measuring temperature was further cooled to 50 °C a crystalline substance was obtained.

Figure 5 presents the temperature-dependent X-ray diffraction diagrams obtained from sample of **2F-14** at 200 and 50 °C. At 200 °C (Figure 5a), two sharp scatterings at 3.08 and 6.09° are observed that correspond to a *d* spacing of 28.7 and 14.4 Å. These reflections are in a 1:1/2 ratio, which indicates a lamellar ordering in the mesophase. Only a diffuse scattering around 20° is obtained. These results indicate the formation of a smectic phase at 200 °C; the liquid-crystal state for smectic A, smectic C and smectic F phases show a diffuse outer ring accompanied by a strong inner diffraction as reported previously.[27] The polarizing optical microscopy (Figure 2a) revealed a lamellar smectic A for **2F-14** in

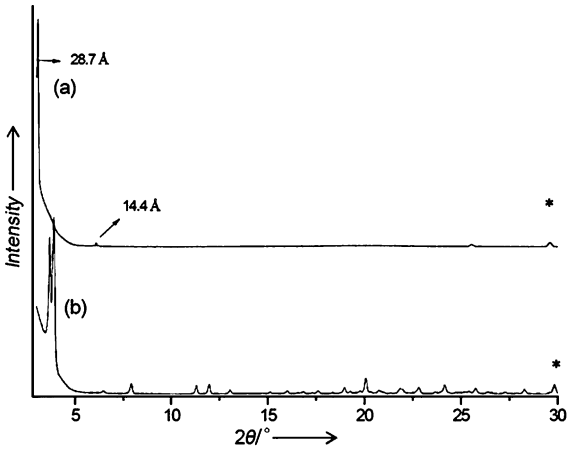

Figure 5. X-ray diffraction pattern of compound **2F-14** at a) 200 and b) 50 °C (before heating). The diffraction peak at $2\theta = 29.7°$ is from the glass sample holder.

this temperature range. Both results are consistent with a smectic A structure. The calculated molecular length of a molecule of **2F-14** is 28.7 Å, and the layer thickness of **2F-14** is larger than the molecular length ($d/l = 1.07$; see Table 4) but significantly smaller than twice the length, thus indicating bilayer structures. The diffraction plot measured at 50 °C (Figure 5c) demonstrates that the smectic A phase has been quenched at this temperature.

Table 4. X-ray diffraction analysis data of the compounds.

Compound	*T* [°C]	*d*1 [Å]	*d*2 [Å]	*d*3 [Å]	*l* [Å][a]	Ratio *d*1/*l*	Phase
5F-14	150	26.1	8.7	6.5	28.2	0.93	SmA
6F-14[b]	110	27.8	18.0	6.7	27.4	1.01	SmA
7F-14[b]	170	24.4	8.2	–	26.7	0.91	SmA
2F-14[b]	200	28.7	14.4	–	26.7	1.07	SmA

[a] Molecular length (*l*) was calculated for the fully extended conformation (estimated with Gaussian 03). [b] See the Supporting Information.

Thermal Stability

Thermal stabilities, which range from 245 to 273 °C were affected by the terminal N-heterocycle, and the substituent group on the imidazole investigated by thermogravimetric analysis, which measures decomposition by weight loss. Data shown in Table 3 indicate that the decomposition temperatures for these compounds, (**5**–**7**)**H-14/18**, (**5**–**7**)**F-14/18**, **2F-14/18**, **5F-14/18B**, were higher than the clearing points. The decomposition temperatures were correlated with the structures of the N-heterocyclic (C5–C7) imidazolium salts (Figure 6). In general, the new compounds with fluorinated N-heterocyclic imidazolium salts and a carbon number of 14 were thermally more stable than those constructed from compounds with a carbon number of 18. However, the new compounds with nonfluorinated N-heterocyclic imidazolium and a carbon number of 18 were thermally more stable than those constructed from a carbon number of 14.

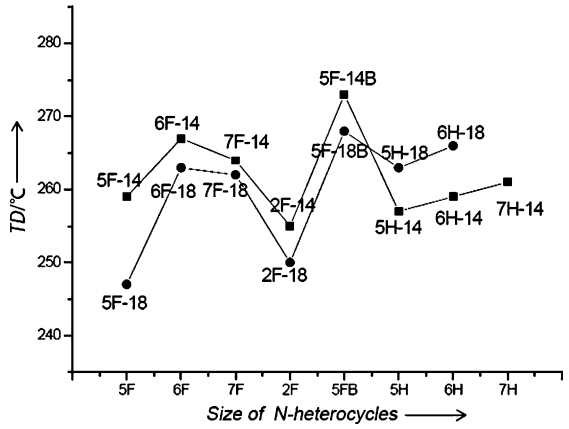

Figure 6. Correlation between thermal stability and the structure of N-heterocyclic (C5–C7) imidazole-based compounds.

The new compounds with a carbon number of 14 and a fluorocarbon N-heterocycle (3,3,4,4-tetrafluoropyrrolidine, 3,3,4,4,5,5-hexafluoropiperidine, 3,3,4,4,5,5,6,6-octafluoroazepane) as terminal group were more stable than those with a hydrocarbon N-heterocycle (pyrrolidine, piperidine, azepane) as terminal group, whereas when the compounds were linked to a carbon number of 18, the stability of these compounds was converse. This suggests that the rigidity of the molecule and the terminal bromoalkane also influences its thermal stability, for example, changing the 3,3,4,4-tetrafluoropyrrolidine to 3,3,4,4,5,5-hexafluoropiperidine leads to a decrease in thermal stability.

UV/Vis Absorption and Photoluminescence Spectroscopy

The UV absorption spectra for solutions of compounds **2F-18** and (**5**–**7**)**F-18** in dichloromethane are presented in Figure 7. Their maximum absorption peaks are collected in Table 5. As the terminal fluorocarbon N-heterocycle size of the compounds increases from a five- to a seven-membered ring, their λ_{max} values show a hypsochromic shift of 12 nm, that is, from 281 nm for **5F-18** to 269 nm for the **7F-18**, but compound **2F-18** shows a bathochromic shift of 3 nm as the terminal fluorocarbon N-heterocycle of the 3,4-difluoropyrrole is altered to 3,3,4,4-tetrafluoropyrrolidine.

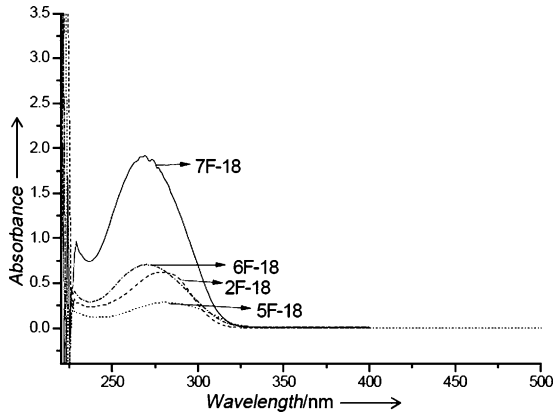

Figure 7. UV/Vis spectra of compounds **2F-18** (dashed line), **5F-18** (dotted line), **6F-18** (dashed-dotted line), and **7F-14** (solid line).

Table 5. UV-visible and fluorescence spectra analysis data of the compounds.

Compound	λ_{max} [nm]	λ_{exc} [nm]	λ_{em} [nm]
2F-18	278	282	389
5F-18	281	286	429
6F-18	270	277	411
7F-18	269	276	402

The emission fluorescence spectra of compounds **2F-18** and (**5**–**7**)**F-18** are given in Figure 8. All spectra were recorded from a dilute solution in dichloromethane (1×10^{-6} mol L^{-1}) at λ_{exc} = 282 nm for **2F-18**, 286 nm for **5F-18**, 277 nm for **6F-18**, and 276 nm for **7F-18** (all values of λ_{exc} were obtained from their excitation spectra). All compounds exhibit strong emission fluorescence from 389 to 429 nm. As the terminal fluorocarbon N-heterocycle size of the compounds increases from a five- to a seven-membered ring, their λ_{em} decreases from 429 to 402 nm. This arises from the fact that with the increase in the number of the electron-withdrawing fluroalkyl groups, the conjugated system is weakened, which contributes to a blueshift in fluorescence.

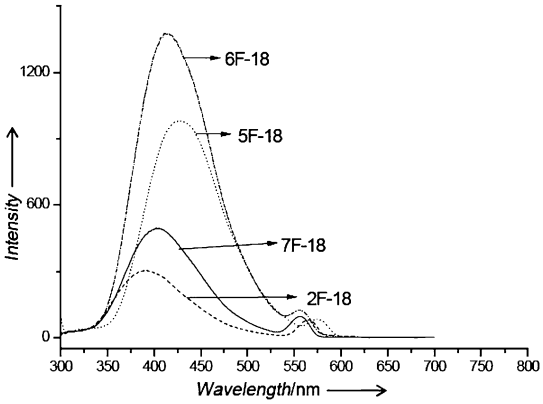

Figure 8. Fluorescence spectra of compounds **2F-18** (dashed line), **5F-18** (dotted line), **6F-18** (dashed-dotted line), and **7F-14** (solid line).

Theoretical Study

Theoretical calculations are of great importance in predicting the structure of ionic liquids.[29] In particular, density functional theory (DFT) calculations have been found to be very useful in predicting the molecular structure as well as interactions present in the molecule.[30–32] DFT computations were performed with Becke's three-parameter hybrid functional and the nonlocal correlation of the Lee–Yang–Parr (B3LYP) method in the gaseous phase.[33] The 6-31+G basis set was used to obtain the geometry optimization of the structures of imidazole-based compounds **M5F**–**M7F** and their related imidazolium-based ILCs, (**5**–**7**)**F-14**, with help of the Gaussian 03 (Revision D.01) suite of programs.[34] The computed structures were visualized by using the GaussView program.[35] Based on the theoretical calculations to measure β (hydrogen bonds) and μ (dipole) for ILCs, it is possible to determine the influence of both cation and anion

structure to obtain a solid background for the following discussion.[36] The conformation expression is mainly a thermodynamic problem, so the total energy of each different conformation can reflect the stability of the structure. For the six-membered-ring N-heterocycle, both **M6F** and **6F-14** have two different conformations, chair and boat forms, with their total energies being −1303.05774883, −4425.52048797 and −1303.05088990, −4425.510124206 a.u. The total molecular energy of the boat form was larger than that of the chair form by approximately 18.01 and 27.21 kJ mol^{-1} (1 a.u. = 2625.51 kJ mol^{-1}), respectively, thus indicating that the chair conformation of the terminal 3,3,4,4,5,5-hexafluoropiperidine compound is more stable than the boat conformation from a thermodynamic point of view. Thus the terminal 3,3,4,4,5,5-hexafluoropiperidine compound should exist in the chair conformation. In comparison with 3,3,4,4,5,5-hexafluoropiperidine (C6) and 3,3,4,4-tetrafluoropyrrolidine (C5), the 3,3,4,4,5,5,6,6-octafluoroazepane (C7) adopts the twisted-boat conformation, which decreases the molecular ordered arrangement from a five- to a seven-membered ring. On the basis of their appearance, the reported imidazolium salts can be classified into three different types: rod, V, and U shapes.[36] To estimate the degree of deviation from linearity, the angle (see Table 6, $\measuredangle a$, $\measuredangle b$, $\measuredangle c$) is defined by the center imidazolium ring and the connected two arms. The V shape of the cation was observed for ILCs (**5**–**7**)**F-14**. The angles in the V-shaped systems span a range from 159 to 161°: **5F-14** ($\measuredangle a$ = 159.077°), **6F-14** ($\measuredangle b$ = 160.577°), and **7F-14** ($\measuredangle c$ = 160.449°). This shows that the mesomorphic behavior is dominated by the size of the N-heterocycle ring and the angles in the V-shaped systems

Imidazole-based compounds **M6F** and **M7F** melted into an isotropic liquid at 82.1 and 115.7 °C directly with no observed liquid-crystal texture. The range of mesomorphic phases for their related imidazolium-based ILCs **5F-14**, **6F-14**, and **7F-14** first decreases and then increases as the terminal N-heterocycle size increases. This can be explained by the geometrical parameters (Figure 9) in which the coplanar structure of the molecule is destroyed upon expansion of the terminal N-heterocycle, which is manifested in their dihedral angles and bond angles (Table 6) and comes about as a result of the structures of these molecules, thereby leading to a change in the number of intermolecular interactions. By comparing the geometry optimization of the structures of imidazole-based compounds, **M5**–**7F**, and their related imidazolium-based ILCs, (**5**–**7**)**F-14**, it shows three factors that affect the dipole moment including: 1) the size of the N-heterocycle ring, 2) the fluoroalkyl substituent on the heterocycle, and 3) the different alkyl chains on the cation. The existence of a high dipole moment in the liquid-crystal molecule favorably boosts the inter- and intramolecular interaction and influences mesomorphic behavior. Consequently, these factors result in the diversity of the liquid-crystalline phase range and clearing point among these compounds.

Evaluation of the Influence of the Nonionic Imidazoles and Ionic Imidazolium

In contrast to the series of noncharged imidazoles, fluorocarbon and hydrocarbon N-heterocyclic imidazolium ionic liquid crystals have a broader range of mesomorphic phases, some of which exhibit different phase types (e.g., **M5H** (Cr

Table 6. Geometrical parameters of **M5**–**7F** and (**5**–**7**)**F-14** calculated with Gaussian 03.

Comp	Dihedral angles [°]		Bond angles [°]		Dipole moment [Debye]	Molecular length [10^{-1} nm]	Hydrogen bonds H···Br [10^{-1} nm]
	C1-C6-N26-C19	−5.274	C6-N26-C19	123.193			
M5F	C6-N26-C19-C23	−168.988	C3-N11-C12	126.651	2.147	12.181	
	C4-C3-N11-C13	−42.940					
	C1-C6-N28-C19	−46.029	C6-N28-C19	121.815			
M6F	C6-N28-C19-C21	−107.665	C3-N11-C12	126.607	2.903	12.083	
	C4-C3-N11-C13	−40.198					
	C1-C6-N28-C11	4.230	C6-N28-C11	122.700			
M7F	C6-N28-C11-C13	93.900	C3-N21-C2	126.743	5.921	12.091	
	C4-C3-N21-C22	−41.008					
	C2-C1-N7-C11	−5.215	C1-N7-C11	123.269			
	C1-N7-C11-C10	−169.261	C4-N24-C25	123.966			
5F-14	C3-C4-N24-C26	42.105	C28-N40-C31	127.930	10.960	28.195	2.298
	C28-N40-C31-C32	−105.015	C4-N24-N40	159.077 ($\measuredangle a$)			
	C6-C1-N72-C64	43.349	C1-N72-C64	121.956			
	C1-N72-C64-C68	108.577	C4-N11-C12	124.766			
6F-14	C5-C4-N11-C12	−28.085	C12-N27-C18	123.574	10.677	27.425	2.218
	C12-N27-C18-C19	70.130	C4-N11-N27	160.577 ($\measuredangle b$)			
	C6-C1-N73-C63	−15.041	C1-N73-C63	122.274			
	C1-N73-C63-C65	98.315	C4-N11-C13	126.263			
7F-14	C5-C4-N11-C13	−33.341	C15-N27-C18	126.702	10.407	26.658	2.213
	C15-N27-C18-C19	−103.061	C4-N11-N27	160.449 ($\measuredangle c$)			

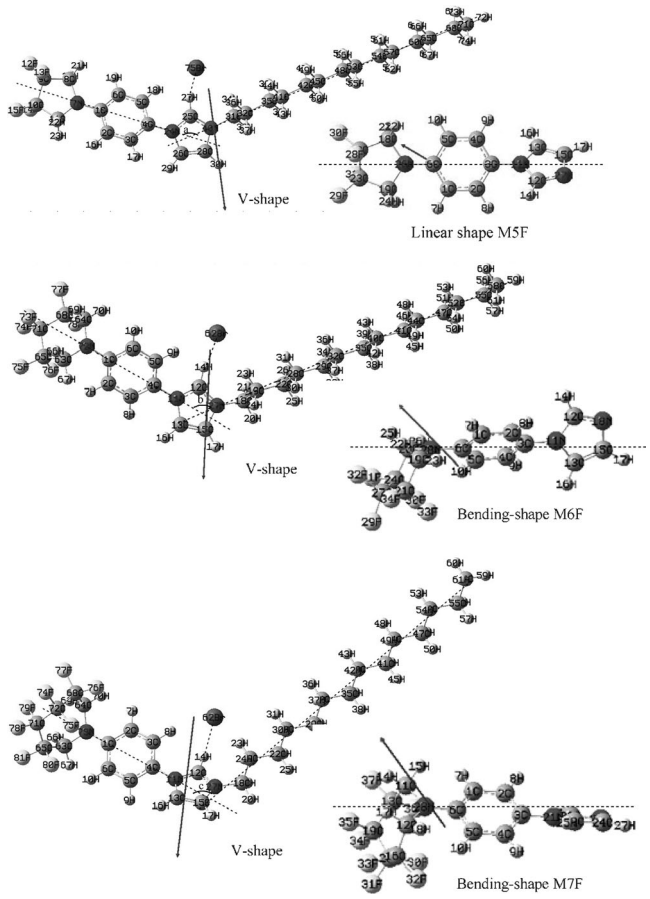

Figure 9. The optimized geometry of **M5F**–**M7F** and corresponding ionic liquid crystals (**5**–**7**)**F-14**.

178.9 °C SmE 187.9 °C), **5H-14** (Cr 100.8 °C SmA 123.9 °C)). The nonionic imidazoles **M6F** and **M7F** melted directly into an isotropic liquid at 82.1 and 115.7 °C with no liquid-crystal texture observed. But the corresponding ionic imidazolium compounds, **6H-14/18** and **7F-14/18**, have a broad smectic A. The additional attractive electrostatic interactions provided by the charged polar groups and polar–apolar interface force effectively increases the polarizability anisotropy and rigidity of the molecule, hence influencing the mesophase behavior, melting point, and the clearing point. For example, the μ (dipole) parameters of noncharged imidazoles **M5F** increase from 2.147 to 10.960 Debye after quaternization with appropriate 1-bromotetradecane. The large μ (dipole) of ionic liquids is attributed to two cumulative effects: the ion-pairing strength and the individual polarizabilities of both the cation and anion. This is shown by the influence of anion and cation structures (alkyl chain length of R) on the dipolarity/polarizability.[37] Thus, the additional charged polar groups are beneficial to the formation of a lamellar liquid-crystal phase.

Influence of the Terminal N-Heterocycle

The effect of the terminal N-heterocycle on the melting point, transition temperatures, mesophase morphology, UV/Vis spectra, and fluorescence spectra of the liquid crystals was investigated. Compared with nonfluorinated N-heterocyclic compounds, fluorinated N-heterocyclic compounds differ in terms of transition temperatures and mesophase morphology. For example, fluorinated N-heterocyclic compounds have a broader mesophase range (e.g., **5F-18** (Cr 108.3 °C SmA 165.3 °C), **5H-18** (Cr′ 111.7, SmA 121.5 °C), **6F-18** (Cr 107.5 °C SmA 116.2 °C), **6H-18** (Cr 61.2 °C SmA 71.8 °C)). However, among nonionic imidazoles, hydrocarbon N-heterocyclic nonionic imidazoles have a broader mesophase range than fluorocarbon N-heterocyclic imidazole (e.g., **M5H** (Cr 178.9 °C SmE 187.9 °C), **M5F** (Cr 175.4 °C SmE 178.0)); **M6F** and **M7F** melted directly into an isotropic liquid at 82.1 and 115.7 °C with no liquid-crystal texture observed. The low polarizability of fluorine shows the weak intermolecular forces of perfluoro systems, which results in very low surface tensions of liquids. The strong inductive effect of the C–F bond on the N-heterocycle-polarized C–H bond enables the hydrogen to be involved in hydrogen bonding with the fluorine of a neighboring molecule.[38]

Any unit that protrudes from the side of the mesogenic core can result in a disruption in the intermolecular forces of attraction and molecular packing. The larger size of the fluoro substituent clearly affects the smectic phase stability, therefore hydrocarbon N-heterocyclic nonionic imidazoles have a broader mesophase range. However, for the imidazolium in V-shaped systems, in general, the terminal N-heterocycle relative to the molecule is small, and only the fluoro substituent is small enough to preserve reasonable liquid crystallinity. Therefore, although a fluoro substituent clearly causes a steric effect, the size influence is not too drastic, which enables it to be usefully incorporated into parent molecules for beneficial modification of imidazolium properties. As the terminal N-heterocycle size increases from a five- to a seven-membered ring, the range of hydrocarbon N-heterocyclic compounds narrows rapidly (e.g., **5H-14** (Cr 100.8 °C SmA 123.9 °C), **6H-14** (Cr 64.1 °C SmA 69.6 °C)); **7H-14** is an isotropic liquid at 36.8 °C with no liquid-crystal texture observed, whereas the range of fluorocarbon N-heterocyclic compounds first decreases and then increases as the terminal N-heterocycle size increases (e.g., **5F-14** (Cr 89.1 °C SmA 157.2 °C), **6F-14** (Cr 106.0 °C SmA 112.3 °C), **7F-14** (Cr′ 148.7, SmA 180.4 °C)). This might be because with the increase in the terminal N-heterocycle, the coplanar structure of the molecule is destroyed. However, the increase also induces a change in shape types and the width of the molecule, thereby increasing the distance between molecules and resulting in a decrease in the number of intermolecular interactions. These factors lead to a change in both the liquid-crystalline phase ranges and the clearing point (Scheme 7).

Conclusion

A series of novel fluorocarbon and hydrocarbon N-heterocyclic imidazole-based liquid crystals (LCs) and related imi-

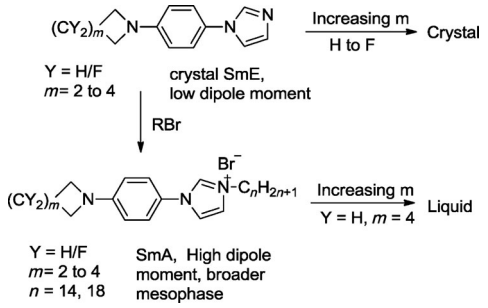

Scheme 7. The structure–property relationship of N-heterocyclic LCs and ILCs.

dazolium-based ionic liquid crystals (ILCs) have been prepared in good yield through Ullmann-type coupling and Debus–Radziszewski imidazole synthesis. The structure–property relationship of these new liquid-crystal compounds is shown in Scheme 7. Their melting points, decomposition temperatures, clearing points, mesomorphism types, and fluorescence were determined. Their mesomorphic behavior and physicochemical properties are adjusted by altering the polarity of the terminal N-heterocycle. The nonionic imidazole **M5F** with the terminal 3,3,4,4-tetrafluoropyrrolidine ring adopted a distorted N1-envelope conformation that shows a mosaic texture of a crystal smectic E phase, and the hydrocarbon nonionic imidazoles also exhibited the mosaic texture of the crystal smectic E phase, whereas fluorocarbon and hydrocarbon N-heterocyclic imidazolium ionic salts displayed disordered SmA mesophases. They have a broader smectic phase range than nonionic imidazole compounds. Some of these compounds have relatively low melting points but high clearing temperatures (e.g., **7F-18** (Cr 80.2 °C SmA 182.3 °C)). Fluorocarbon N-heterocyclic imidazolium ionic compounds exhibit strong emission fluorescence (e.g., **5F-18** ($\lambda_{em}=429$ nm)). These fluorocarbon and hydrocarbon N-heterocyclic imidazole-based liquid crystals exhibit good thermal stabilities, broad smectic phase ranges, high dipole moments, relatively low melting points, but high clearing points and strong emission fluorescence. Therefore the imidazole unit is an excellent platform that can be designed to promote liquid-crystalline phases. When comparing the mesomorphic behavior and physicochemical properties between nonionic (neutral) liquid crystals and ionic liquid crystals in this work, the N-heterocyclic imidazolium-based ionic liquid crystals display the highest dipole moment (**5F-14**, $\mu=10.96$ Debye) and the broadest smectic phase range (**5F-14B**, Cr 84.1 °C SmA 251.5 °C), which indicates that these N-heterocyclic imidazolium-based ionic liquid crystals can be used as components to ensure the stability of certain smectic liquid-crystal states that could be used as new liquid-crystal materials.

Experimental Section

General Considerations

All the reagents were of analytical grade, purchased from commercial sources, and used as received. ^{1}H and ^{19}F NMR spectra were recorded with a 400 MHz spectrometer operating at 400 and 376 MHz, respectively. Chemical shifts are reported relative to Me_4Si for ^{1}H, and CCl_3F for ^{19}F; the solvent was $CDCl_3$ unless otherwise specified. TGA measurements were performed at a heating rate of 10 °C min^{-1} with a Netzsch STA409PC (Germany) instrument. DSC plots were recorded at a scan rate of 5 °C min^{-1} with a Netzsch DSC200PC apparatus. Optical micrographs were observed with a polarizing optical microscope (Nikon LINKAM-THMSE600) equipped with a heating plate (HCS601). Variable-temperature X-ray diffraction experiments were performed with a Bruker D8 Avance X-ray diffractometer (using $Cu_{K\alpha1}$ radiation at a wavelength of 1.54 Å) equipped with a temperature controller. UV/Vis spectra were recorded with a JASCO UV-530 instrument. Fluorescence spectra were recorded with a Hitachi LTD spectrophotometer. Elemental analyses were performed with an EXETER CE-440 instrument.

*General Procedure for the Preparation of Iodobenzene N-Heterocycle Compounds (**I5–7H, I5–6F**)*

Trifluoromethanesulfonic acid polyfluoroalkyldiyl (**1f–2f**) and 4-toluene sulfonyl alkyldiyl (**1h–3h**) (1 mmol), 4-iodobenzenamine (1 mmol, 219.02 mg), triethylamine (2 mL), and ethanol (2 mL) were placed in a Pyrex glass tube, sealed, heated at 90 °C for 24 h, and then allowed to cool to room temperature. The crude product was added to dichloromethane (50 mL), then washed with water (3×30 mL) and dried over anhydrous sodium sulfate. The solvent was removed under vacuum, and the residue was purified by chromatography on silica gel to give the target product. $R_f=0.3$ (petroleum).

3,3,4,4-Hetrafluoro-1-(4-iodophenyl)pyrrolidine (**I5F**), yield: 78 %. ^{1}H NMR (400 MHz, $CDCl_3$): $\delta=7.55$ (d, $J=8.8$ Hz, 2H), 6.31 (d, $J=8.8$ Hz, 2H), 3.78 ppm (m, 4H); ^{19}F NMR (376 MHz, $CDCl_3$): $\delta=-110.83$–-129.53 ppm (m, 1H); MS (ESI): m/z calcd for $C_{10}H_8F_4IN$: 344.96 [M^+]; found: 344.83; elemental analysis calcd (%) for $C_{10}H_8F_4IN$: C 34.81, H 2.34, N 4.06; found: C 34.79, H 2.33, N 4.05.

3,3,4,4,5,5-Hexafluoro-1-(4-iodophenyl)piperidine (**I6F**), yield: 75 %. ^{1}H NMR (400 MHz, $CDCl_3$): $\delta=7.59$ (d, $J=8.3$ Hz, 2H), 6.72 (d, $J=8.4$ Hz, 2H), 3.72 ppm (t, $J=8.1$ Hz, 4H); ^{19}F NMR (376 MHz, $CDCl_3$): $\delta=-123.54$ (s, 4F), -139.30 ppm (s, 2F); MS (ESI): m/z: 582.2 [$M+NH_4^+$]$^+$; elemental analysis calcd (%) for $C_{11}H_8F_6IN$: C 33.44, H 2.04, N 3.55; found: C 33.46, H 2.16, N 3.50.

*First Synthetic Route: General Procedure for the Preparation of N-Heterocyclic Imidazolium (**M5H–M7H, MNH$_2$, M2F**)*

1) Aryl iodine (1.0 mmol), imidazole (0.081 g, 1.2 mmol), CuI (9.5 mg, 0.05 mmol), (nBu)$_4$NBr (16 mg, 0.05 mmol), NaOH (80 mg, 2 mmol), and DMSO (5 mL) were placed in a Pyrex glass tube and sealed, then stirred at 120 °C for 40 h. Then the reaction mixture was diluted with CH_2Cl_2 (30–40 mL), washed with water (3×30 mL), then dried over anhydrous sodium sulfate. The solvent was removed under vacuum, and the residue was purified by chromatography on silica gel to give the target product. $R_f=0.4$ (PE/EtOAc = 1:2).

2) CuI (38.4 mg, 0.2 mmol), K_3PO_4 (0.422 g, 2.0 mmol), imidazole (0.095 g, 1.4 mmol), aryl iodine (1.0 mmol), and DMF (2 mL) were placed in a Pyrex glass tube and sealed, then stirred at 120 °C for 40 h. Then the reaction mixture was filtered through Celite (2.5 g), the solution was diluted with CH_2Cl_2 (30–40 mL), washed with water (3×30 mL), and dried over anhydrous sodium sulfate. The solvent was removed under vacuum, and the residue was purified by chromatography on silica gel to give the target product. $R_f=0.4$ (PE/EtOAc = 1:2).

1-[4-(Pyrrolidin-1-yl)phenyl]-1*H*-imidazole (**M5H**), yield 1: 56 %, yield 2: 90 %. ^{1}H NMR (400 MHz, $CDCl_3$): $\delta=7.72$ (s, 1H), 7.22 (d, $J=8.9$ Hz, 2H), 7.17 (d, $J=6.7$ Hz, 2H), 6.59 (d, $J=8.9$ Hz, 2H), 3.31 (t, $J=6.6$ Hz, 4H), 2.11–1.98 ppm (m, 4H); MS (EI) m/z: 213.2 (100); elemental analy-

sis calcd (%) for $C_{13}H_{15}N_3$: C 73.21, H 7.09, N 19.70; found: C 73.46, H 7.16, N 19.50.

1-[4-(Piperidin-1-yl)phenyl]-1*H*-imidazole (**M6H**), yield 1: 57%, yield 2: 91%. ^{1}H NMR (400 MHz, $CDCl_3$): δ = 8.01 (s, 1H), 7.27 (d, J = 7.4 Hz, 3H), 6.98 (d, J = 7.8 Hz, 3H), 3.24–3.16 (m, 4H), 2.96 (s, 3H), 2.88 ppm (s, 3H); MS (EI): m/z: 227.2 (100); elemental analysis calcd (%) for $C_{14}H_{17}N_3$: C 73.98, H 7.54, N 18.49; found: C 73.90, H 7.47, N 17.96.

1-[4-(Azepan-1-yl)phenyl]-1*H*-imidazole (**M7H**), yield 1: 56%, yield 2: 89%. ^{1}H NMR (400 MHz, $CDCl_3$): δ = 7.85 (s, 1H), 7.31–7.14 (m, 4H), 6.73 (m, 2H), 3.49 (m, 4H), 1.81 (s, 4H), 1.57 ppm (d, J = 1.4 Hz, 4H); MS (EI): m/z: 241.3 (100); elemental analysis calcd (%) for $C_{15}H_{19}N_3$: C 74.65, H 7.94, N 17.41; found: C 74.58, H 7.95, N 17.42.

4-(1*H*-Imidazol-1-yl)aniline (**MNH$_2$**), yield 1: 57%, yield 2: 90%. ^{1}H NMR (400 MHz, DMSO): δ = 7.97 (s, 1H), 7.50 (s, 1H), 7.23 (d, J = 7.9 Hz, 2H), 7.03 (s, 1H), 6.65 (d, J = 7.9 Hz, 2H), 5.30 ppm (s, 2H).

1-[4-(3,4-Difluoro-1*H*-pyrrol-1-yl)phenyl]-1*H*-imidazole (**M2F**), yield 1: 58%, yield 2: 93%. ^{1}H NMR (400 MHz, $CDCl_3$): δ = 7.85 (s, 1H), 7.46 (d, J = 7.1 Hz, 2H), 7.38 (d, J = 8.8 Hz, 2H), 7.27 (d, J = 6.2 Hz, 2H), 7.23 (s, 2H), 6.76 ppm (d, J = 1.0 Hz, 2H); ^{19}F NMR (376 MHz, $CDCl_3$): δ = −176.33 ppm (s, 2F); MS (EI): m/z: 245.2 (100); elemental analysis calcd (%) for $C_{13}H_9F_2N_3$: C 63.67, H 3.70, N 17.14; found: C 63.79, H 3.80, N 16.78.

Second Synthetic Route

MNH$_2$ (0.159 g, 1 mmol), **1f** and **1h** (1 mmol), triethylamine (2 mL), and ethanol (2 mL) were placed in a Pyrex glass tube, sealed, heated at 90°C for 24 h, and then allowed to cool to room temperature. The crude product was added to dichloromethane (50 mL), then washed with water (3× 30 mL) and dried over anhydrous sodium sulfate. The solvent was removed under vacuum, and the residue was purified by chromatography on silica gel to give the target products **M5H**, yield: 5%, and **M5F**, yield: 2%. R_f = 0.3 (PE/EtOAc = 1:2).

*Third Synthetic Route: General Procedure for the Preparation of Fluorocarbon N-Heterocyclic Anilines (**N5F–N7F**)*

Trifluoromethanesulfonic acid 2,2,3,3-tretrafluoro-1,4-butanediyl ester (**1f**), trifluoromethanesulfonic acid 2,2,3,3,4,4-hexafluoro-1,5-pentanediyl ester (**2f**), or trifluoromethanesulfonic acid 2,2,3,3,4,4,5,5-octofluoro-1,6-hexanediyl ester (**3f**) (1 mmol), *p*-phenylenediamine (2 mmol), Et_3N (5 mmol), and ethanol (25 mL) were placed in a round-bottomed flask fitted with a reflux condenser and heated at reflux for 30 h. After cooling, the solvent was removed under vacuum. The residue was added to dichloromethane (50 mL), then washed with water (3×20 mL) and dried over anhydrous sodium sulfate. The solvent was removed under vacuum, and the residue was purified by chromatography on silica gel to give the target product. R_f = 0.3–0.4 (PE/CH_2Cl_2 = 1:1).

4-(3,3,4,4-Tetrafluoropyrrolidin-1-yl) aniline (**N5F**), yield: 93%. ^{1}H NMR (400 MHz, $CDCl_3$): δ = 6.73–6.66 (m, 2H), 6.47–6.36 (m, 2H), 3.73 (m, 4H), 3.59–2.51 ppm (br, 2H); ^{19}F NMR (376 MHz, $CDCl_3$): δ = −123.04–−123.39 ppm (m, 4F); MS (ESI): m/z: 235.53 $[M+H]^+$; elemental analysis calcd (%) for $C_{10}H_{10}F_4N_2$: C 51.29, H 4.30, N 11.96; found: C,50.77, H 4.48, N 11.79.

4-(3,3,4,4,5,5-Hexafluoropiperidin-1-yl)aniline (**N6F**), yield: 89%. ^{1}H NMR (400 MHz, $CDCl_3$): δ = 6.87–6.78 (m, 2H), 6.70–6.61 (m, 2H), 3.65–3.42 ppm (m, 4H); ^{19}F NMR (376 MHz, $CDCl_3$): δ = −123.32 (s, 4F), −138.88–−140.68 ppm (m, 2F); MS (EI): m/z: 284.2 (100); elemental analysis calcd (%) for $C_{11}H_{10}F_6N_2$: C 46.49, H 3.55, N 9.86; found: C 46.84, H 3.55, N 9.85.

4-(3,3,4,4,5,5,6,6-Octafluoroazepan-1-yl)aniline (**N7F**), yield: 86%. ^{1}H NMR (400 MHz, $CDCl_3$): δ = 6.82 (d, J = 8.5 Hz, 2H), 6.65 (d, J = 8.6 Hz, 2H), 3.89 (t, J = 12.7 Hz, 4H), 2.63 ppm (br, 2H); ^{19}F NMR (376 MHz, $CDCl_3$): δ = −113.30 (s, 4F), −128.40 ppm (s, 4F); MS (ESI): m/z: 335.58 $[M+H]^+$; elemental analysis calcd (%) for $C_{12}H_{10}F_8N_2$: C 43.13, H 3.02, N 8.38; found: C 42.98, H 3.38, N 8.07.

*General Procedure for the Preparation of N-Heterocyclic Imidazolium (**M5F–M7F**)*

N-Heterocyclic aniline (0.01 mol), MeOH (5 mL), and 40% aqueous glyoxal (1.74 g, 0.012 mol) were placed in a three-necked round-bottomed flask and stirred at room temperature for 16 h to form a yellow mixture. NH_4Cl (1.07 g, 0.02 mol) was added followed by 37% aqueous formaldehyde (1.62 g, 0.02 mol). The mixture was diluted with MeOH (40 mL) and heated to reflux for 1 h. H_3PO_4 (1.4 mL, 85%) was added slowly over 10 min. The resulting mixture was then stirred at reflux for another 8 h. After removal of the solvent under vacuum, the dark residue was poured onto ice (30 g) and neutralized with 40% aqueous KOH solution until the solution was at pH 9. The resulting mixture was extracted with dichloromethane (3×30 mL). The organic phases were washed with water (3×30 mL) and dried over anhydrous sodium sulfate. The solvent was removed under vacuum, and the residue was purified by chromatography on silica gel to give the target product. R_f = 0.4 (PE/EtOAc = 1:2).

1-[4-(3,3,4,4-Tetrafluoropyrrolidin-1-yl)phenyl]-1*H*-imidazole (**M5F**), yield: 85%. ^{1}H NMR (400 MHz, $CDCl_3$): δ = 8.67 (s, 1H), 7.45 (d, J = 8.7 Hz, 2H), 7.38 (s, 1H), 7.31 (s, 1H), 6.65 (d, J = 8.7 Hz, 2H), 3.89 ppm (m, 4H); ^{19}F NMR (376 MHz, $CDCl_3$): δ = −122.91 ppm (m, 4F); MS (EI): m/z: 285.2 (100); elemental analysis calcd (%) for $C_{13}H_{11}F_4N_3$: C 54.74, H 3.89, N 14.73; found: C 54.69, H 3.91, N 14.52.

1-[4-(3,3,4,4,5,5-Hexafluoropiperidin-1-yl)phenyl]-1*H*-imidazole (**M6F**), yield: 84%. ^{1}H NMR (400 MHz, $CDCl_3$): δ = 7.78 (s, 1H), 7.33 (d, J = 8.9 Hz, 2H), 7.21 (d, J = 9.3 Hz, 2H), 7.05 (d, J = 8.9 Hz, 2H), 3.92–3.72 ppm (m, 4H); ^{19}F NMR (376 MHz, $CDCl_3$): δ = −123.52 (s, 4F), −139.27 ppm (s, 2F); MS (EI): m/z: 149.1 (100); elemental analysis calcd (%) for $C_{14}H_{11}F_6N_3$: C 50.16, H 3.31, N 12.53; found: C 50.34, H 3.36, N 12.38.

1-[4-(3,3,4,4,5,5,6,6-Octafluoroazepan-1-yl)phenyl]-1*H*-imidazole (**M7F**), yield: 80%. ^{1}H NMR (400 MHz, $CDCl_3$): δ = 7.77 (s, 1H), 7.34 (d, J = 2.1 Hz, 2H), 7.20 (d, J = 7.7 Hz, 2H), 7.03 (d, J = 9.1 Hz, 2H), 4.12 ppm (t, J = 12.2 Hz, 4H); ^{19}F NMR (376 MHz, $CDCl_3$): δ = −112.38–−112.63 (m, 4F), −128.50 ppm (s, 4F); MS (EI): m/z: 385.2 (100); elemental analysis calcd (%) for $C_{15}H_{11}F_8N_3$: C 46.76, H 2.88, N 10.91; found: C 47.07, H 3.00, N 10.64.

*General Procedure for the Preparation of N-Heterocyclic Imidazolium-Based ILCs ((**5–7**)**H-14**, (**5–6**)**H-18**, **2F-14/18**, (**5–7**)**F-14/18**)*

N-Heterocyclic imidazole (1 mmol) and 1-bromotetradecane (1.386 g, 5 mmol) or 1- bromohexadecane bromide (1.661 g, 5 mmol) and acetonitrile (8 mL) were placed in a Pyrex glass tube and sealed, then stirred at 120°C for 18 h. The solvent was removed under vacuum, and the residue was purified by chromatography on silica gel to give the target product. R_f = 0.2–0.4 (EtOAc/MeOH = 10:1).

1-Tetradecyl-3-[4-(pyrrolidin-1-yl)phenyl]-1*H*-imidazolium bromide (**5H-14**), yield: 82%. ^{1}H NMR (400 MHz, $CDCl_3$): δ = 10.76 (s, 1H), 7.53 (d, J = 9.0 Hz, 2H), 7.45 (d, J = 1.6 Hz, 1H), 7.39 (s, 1H), 6.60 (d, J = 9.0 Hz, 2H), 4.56 (t, J = 7.4 Hz, 2H), 3.39–3.24 (m, 4H), 2.11–2.00 (m, 4H), 2.02–1.90 (m, 2H), 1.45–1.15 (m, 22H), 0.88 ppm (t, J = 6.9 Hz, 3H); MS (ESI): m/z: $[M-Br^-]^+$; elemental analysis calcd (%) for $C_{27}H_{44}BrN_3{\cdot}0.5\,H_2O$: C 64.91, H 9.08, N 8.41; found: C 65.19, H 8.94, N 8.35.

1-Octadecyl-3-[4-(pyrrolidin-1-yl)phenyl]-1*H*-imidazolium bromide (**5H-18**), yield: 80%. ^{1}H NMR (400 MHz, $CDCl_3$): δ = 10.80 (s, 1H), 7.52 (d, J = 9.0 Hz, 2H), 7.41 (s, 1H), 7.33 (s, 1H), 6.61 (d, J = 7.2 Hz, 2H), 4.57 (t, J = 7.4 Hz, 2H), 3.31 (t, J = 6.6 Hz, 4H), 2.22–1.84 (m, 6H), 1.45–1.20 (m, 32H), 0.88 ppm (t, J = 6.8 Hz, 3H); MS (ESI): m/z: 466.2 $[M-Br^-]^+$; elemental analysis calcd (%) for $C_{31}H_{52}BrN_3{\cdot}H_2O$: C 65.94, H 9.64, N 7.44; found: C 66.39, H 9.35, N 7.42.

1-Tetradecyl-3-[4-(piperidin-1-yl)phenyl]-1*H*-imidazolium bromide (**6H-14**), yield: 78%. ^{1}H NMR (400 MHz, $CDCl_3$): δ = 10.75 (s, 1H), 7.60 (d, J = 9.1 Hz, 3H), 7.50 (d, J = 6.7 Hz, 1H), 7.01 (d, J = 8.8 Hz, 2H), 4.55 (t, J = 7.2 Hz, 2H), 3.35–3.14 (m, 4H), 2.05–1.87 (m, 2H), 1.67 (dd, J = 26.2, 4.6 Hz, 6H), 1.43–1.17 (m, 22H), 0.88 ppm (t, J = 6.8 Hz, 3H); MS (ESI): m/z: 424.2 $[M-Br^-]^+$; elemental analysis calcd (%) for $C_{28}H_{46}BrN_3{\cdot}H_2O$: C 64.35, H 9.26, N 8.04; found: C 64.81, H 8.92, N 7.89.

1-Octadecyl-3-[4-(piperidin-1-yl)phenyl]-1*H*-imidazolium bromide (**6H-18**), yield: 77%. ^{1}H NMR (400 MHz, $CDCl_3$): δ = 10.91 (s, 1H), 7.64 (d, J = 14.0 Hz, 2H), 7.50 (s, 1H), 7.35 (d, J = 2.0 Hz, 1H), 7.13 (s, 2H), 4.57 (t, J = 8.6 Hz, 2H), 3.40 (m, 4H), 3.33–3.24 (m, 4H), 2.03–1.93 (m, 3H), 1.76 (s, 5H), 1.39 (m, 20H), 0.88 ppm (t, J = 6.7 Hz, 9H); MS (ESI): m/z: 480.2 $[M-Br^-]^+$; elemental analysis calcd (%) for $C_{32}H_{54}BrN_3 \cdot H_2O$: C 64.41, H 9.75, N 7.26; found: C 64.09, H 9.38, N 7.32.

1-Tetradecyl-3-[4-(azepan-1-yl)phenyl]-1*H*-imidazolium bromide (**7H-14**), yield: 74%. ^{1}H NMR (400 MHz, $CDCl_3$): δ = 10.76 (s, 1H), 7.55 (d, J = 8.3 Hz, 2H), 7.48 (s, 1H), 7.38 (s, 1H), 6.82 (d, J = 8.7 Hz, 2H), 4.56 (t, J = 7.8 Hz, 2H), 3.71–3.26 (m, 4H), 2.02–1.92 (m, 3H), 1.80 (s, 6H), 1.41–1.23 (m, 23H), 0.88 ppm (t, J = 6.4 Hz, 3H); ^{13}C NMR (101 MHz, $CDCl_3$): δ = 151.31, 134.78, 122.82, 122.37, 120.43, 111.85, 105.10, 50.28, 49.50, 31.88, 30.37, 29.89–28.72 (multicarbon in alkyl chain), 27.14, 26.81, 26.22, 22.62, 14.06 ppm; MS (ESI): m/z: 438.2 $[M-Br^-]^+$; HRMS (EI): m/z calcd for $C_{29}H_{48}N_3$: 438.3853; found: 438.3843.

1-Tetradecyl-3-[4-(3,4-difluoro-1*H*-pyrrol-1-yl)phenyl]-1*H*-imidazolium bromide (**2F-14**), yield: 83%. ^{1}H NMR (400 MHz, $CDCl_3$): δ = 11.33 (s, 1H), 7.95 (d, J = 8.8 Hz, 2H), 7.60 (s, 1H), 7.48 (d, J = 8.8 Hz, 2H), 7.40 (s, 1H), 6.79 (s, 2H), 4.56 (t, J = 9.0 Hz, 2H), 2.07–1.95 (m, 2H), 1.45–1.21 (m, 22H), 0.88 ppm (t, J = 6.7 Hz, 3H); ^{19}F NMR (376 MHz, $CDCl_3$): δ = −175.07 ppm (s, 1F); MS (ESI): m/z: 442.1 $[M-Br^-]^+$; elemental analysis calcd (%) for $C_{27}H_{38}BrF_2N_3 \cdot 2H_2O$: C 58.06, H 7.58, N 7.52; found: C 58.28, H 7.19, N 7.19.

1-Octadecyl-3-[4-(3,4-difluoro-1*H*-pyrrol-1-yl)phenyl]-1*H*-imidazolium bromide (**2F-18**), yield: 84%. ^{1}H NMR (400 MHz, $CDCl_3$): δ = 11.17 (s, 1H), 7.95 (d, J = 8.9 Hz, 2H), 7.76–7.54 (m, 1H), 7.46 (d, J = 4.9 Hz, 3H), 6.79 (s, 2H), 4.54 (d, J = 5.6 Hz, 2H), 2.20–1.87 (m, 2H), 1.57–1.04 (m, 30H), 0.88 ppm (t, J = 6.7 Hz, 3H); ^{19}F NMR (376 MHz, $CDCl_3$): δ = −175.12 ppm (d, J = 10.8 Hz, 2F); MS (ESI): m/z: 498.1 $[M-Br^-]^+$; elemental analysis calcd (%) for $C_{31}H_{46}BrF_2N_3 \cdot 2H_2O$: C 60.58, H 8.20, N 6.84; found: C 60.34, H 7.86, N 6.50.

1-Tetradecyl-3-[4-(3,3,4,4-tetrafluoropyrrolidin-1-yl)phenyl]-1*H*-imidazolium bromide (**5F-14**), yield: 86%. ^{1}H NMR (400 MHz, $CDCl_3$): δ = 11.09 (s, 1H), 7.74 (d, J = 8.9 Hz, 2H), 7.49 (s, 1H), 7.36 (s, 1H), 6.67 (d, J = 8.8 Hz, 2H), 4.55 (t, J = 7.4 Hz, 2H), 3.92–3.82 (m, 4H), 1.99 (m, 2H), 1.43–1.23 (m, 22H), 0.88 ppm (t, J = 6.8 Hz, 3H); ^{19}F NMR (376 MHz, $CDCl_3$): δ = −123.16 ppm (m, 4F); MS (ESI): m/z: 482.1 $[M-Br^-]^+$; elemental analysis calcd (%) for $C_{27}H_{40}BrF_4N_3 \cdot H_2O$: C 55.86, H 7.29, N 7.24; found: C 56.17, H 6.98, N 7.12.

1-Octadecyl-3-[4-(3,3,4,4-tetrafluoropyrrolidin-1-yl)phenyl]-1*H*-imidazolium bromide (**5F-18**), yield: 84%. ^{1}H NMR (400 MHz, $CDCl_3$): δ = 11.10 (s, 1H), 7.74 (d, J = 8.9 Hz, 2H), 7.49 (s, 1H), 7.36 (s, 1H), 6.67 (d, J = 8.8 Hz, 2H), 4.55 (t, J = 7.4 Hz, 2H), 3.88 (m, 4H), 2.07–1.90 (m, 2H), 1.44–1.19 (m, 30H), 0.88 ppm (t, J = 6.8 Hz, 3H); ^{19}F NMR (376 MHz, $CDCl_3$): δ = −123.16 ppm (m, 4F); MS (ESI): m/z: 538.3 $[M-Br^-]^+$; elemental analysis calcd (%) for $C_{31}H_{48}BrF_4N_3$: C 60.19, H 7.82, N 6.79; found: C 59.82, H 7.71, N 6.55.

1-Tetradecyl-3-[4-(3,3,4,4,5,5-hexafluoropiperidin-1-yl)phenyl]-1*H*-imidazolium bromide (**6F-14**), yield: 84%. ^{1}H NMR (400 MHz, $CDCl_3$): δ = 10.98 (s, 1H), 7.78 (d, J = 9.0 Hz, 2H), 7.65 (s, 1H), 7.46 (s, 1H), 7.10 (d, J = 9.0 Hz, 2H), 4.52 (t, J = 7.4 Hz, 2H), 3.88 (t, J = 7.5 Hz, 4H), 2.03–1.92 (m, 2H), 1.30 (m, 22H), 0.88 ppm (t, J = 6.8 Hz, 3H); ^{19}F NMR (376 MHz, $CDCl_3$) δ = −123.63 (s, 4F), −139.11 ppm (s, 2F); MS (ESI): m/z: 532.2 $[M-Br^-]^+$; elemental analysis calcd (%) for $C_{28}H_{40}BrF_6N_3 \cdot H_2O$: C 53.33, H 6.71, N 6.66; found: C 53.87, H 6.51, N 6.61.

1-Octadecyl-3-[4-(3,3,4,4,5,5-hexafluoropiperidin-1-yl)phenyl]-1*H*-imidazolium bromide (**6F-18**), yield: 85%. ^{1}H NMR (400 MHz, $CDCl_3$): δ = 10.95 (s, 1H), 7.78 (d, J = 8.8 Hz, 2H), 7.68 (s, 1H), 7.48 (s, 1H), 7.10 (d, J = 8.9 Hz, 2H), 4.51 (t, J = 7.3 Hz, 2H), 3.88 (s, 4H), 2.04–1.92 (m, 3H), 1.39–1.22 (m, 31H), 0.88 ppm (t, J = 6.7 Hz, 3H); ^{19}F NMR (376 MHz, $CDCl_3$): δ = −123.63 (s, 4F), −139.11 ppm (s, 2F); MS (ESI): m/z: 588.2 $[M-Br^-]^+$; elemental analysis calcd (%) for $C_{32}H_{48}BrF_6N_3 \cdot H_2O$: C 55.97, H 7.34, N 6.12; found: C 56.12, H 7.17, N 5.95.

3-Tetradecyl-1-[4-(3,3,4,4,5,5,6,6-octafluoroazepan-1-yl)phenyl]-1*H*-imidazolium bromide (**7F-14**), yield: 80%. ^{1}H NMR (400 MHz, $CDCl_3$): δ = 11.13 (s, 1H), 7.75 (d, J = 9.1 Hz, 2H), 7.53 (s, 1H), 7.36 (s, 1H), 7.10 (d, J = 9.2 Hz, 2H), 4.54 (t, J = 7.4 Hz, 2H), 4.16 (t, J = 12.0 Hz, 4H), 2.03–1.92 (m, 2H), 1.42–1.22 (m, 22H), 0.88 ppm (t, J = 6.8 Hz, 3H); ^{19}F NMR (376 MHz, $CDCl_3$): δ = −112.24 (m, 4F), −128.48 ppm (s, 4F); MS (ESI): m/z: 582.2 $[M-Br^-]^+$; elemental analysis calcd (%) for $C_{29}H_{40}BrF_8N_3 \cdot H_2O$: C 51.18, H 6.22, N 6.17; found: C 50.99, H 6.07, N 5.91.

3-Octadecyl-1-[4-(3,3,4,4,5,5,6,6-octafluoroazepan-1-yl)phenyl]-1*H*-imidazolium bromide (**7F-18**), yield: 78%. ^{1}H NMR (400 MHz, $CDCl_3$): δ = 11.04 (s, 1H), 7.75 (d, J = 9.0 Hz, 2H), 7.57 (s, 1H), 7.39 (s, 1H), 7.09 (d, J = 9.0 Hz, 2H), 4.53 (t, J = 7.4 Hz, 2H), 4.23 (d, J = 8.7 Hz, 4H), 2.03–1.92 (m, 3H), 1.39–1.22 (m, 29H), 0.91–0.87 ppm (m, 3H); ^{19}F NMR (376 MHz, $CDCl_3$): δ = −112.26 (t, J = 13.2 Hz, 4F), −128.48 ppm (s, 4F); MS (ESI): m/z: 638.2 $[M-Br^-]^+$; elemental analysis calcd (%) for $C_{33}H_{48}BrF_8N_3 \cdot 2H_2O$: C 52.52, H 6.95, N 5.57; found: C 52.82, H 6.83, N 5.91.

*General Procedure for the Preparation of N-Heterocyclic Imidazolium ILCs (**5F-14/18**)*

A solution of 1-tetradecyl-3-[4-(3,3,4,4-tetrafluoropyrrolidin-1-yl)phenyl]-1*H*-imidazolium bromide (562.52 mg, 1 mmol) or 1-octadecyl-3-[4-(3,3,4,4-tetrafluoropyrrolidin-1-yl)phenyl]-1*H*-imidazolium bromide (618.63 mg, 1 mmol) and acetone (8 mL) was placed in a Pyrex glass tube and sealed, then heated to 60 °C. $NaBF_4$ (219.58 mg, 2 mmol) was added and the reaction mixture was heated to reflux for 3 h. Inorganic salts were filtered off and washed with acetone. The solvent was removed under vacuum, and the residue was purified by chromatography on silica gel to give the target product. R_f = 0.2–0.4 (EtOAc/MeOH = 10:1).

1-Tetradecyl-3-[4-(3,3,4,4-tetrafluoropyrrolidin-1-yl)phenyl]-1*H*-imidazolium fluoroborate (**5F-14B**), yield: 82%. ^{1}H NMR (400 MHz, $CDCl_3$): δ = 9.13 (s, 1H), 7.53 (d, J = 8.9 Hz, 3H), 7.43 (s, 1H), 6.64 (d, J = 5.3 Hz, 2H), 4.32 (t, J = 6.3 Hz, 2H), 3.84 (t, J = 8.8 Hz, 4H), 2.00–1.84 (m, 2H), 1.40–1.12 (m, 22H), 0.88 ppm (m, 3H); ^{19}F NMR (376 MHz, $CDCl_3$): δ = −119.53–−126.19 (m, 4F), −151.19 ppm (d, J = 19.6 Hz, 4F); MS (ESI): m/z: 482.6 $[M-Br^-]^+$; elemental analysis calcd (%) for $C_{27}H_{40}BF_8N_3$: C 56.95, H 7.08, N 7.38; found: C 56.52, H 7.53, N 7.54.

1-Octadecyl-3-[4-(3,3,4,4-tetrafluoropyrrolidin-1-yl)phenyl]-1*H*-imidazolium fluoroborate (**5F-18B**), yield: 85%. ^{1}H NMR (400 MHz, $CDCl_3$): δ = 9.18 (s, 1H), 7.55 (m, 4H), 6.67 (m, 2H), 4.35 (m, 2H), 3.88 (t, J = 14.4, 4H), 1.95 (d, J = 20.0 Hz, 3H), 1.51–1.13 (m, 33H), 0.97–0.80 ppm (m, 3H); ^{19}F NMR (376 MHz, $CDCl_3$): δ = −120.64–−125.87 (m, 4F), −151.01 ppm (t, J = 18.8 Hz, 4F); MS (ESI): m/z: 538.8 $[M-Br^-]^+$; elemental analysis calcd (%) for $C_{31}H_{48}BF_8N_3$: C 59.52, H 7.73, N 6.72; found: C 59.82, H 7.52, N 6.54.

Acknowledgements

The authors gratefully acknowledge the support of the National Natural Science Foundation of China (21272080), the Department of Science and Technology, Guangdong Province (2010A020507001-76, 5300410, FIPL-05-003), and the Scientific Research Foundation for the Returned Overseas Chinese Scholars, State Education Ministry.

[1] a) J. W. Goodby, I. M. Saez, S. J. Cowling, V. Görtz, M. Draper, A. W. Hall, S. Sia, G. Cosquer, S. E. Lee, E. P. Raynes, *Angew. Chem. Int. Ed.* **2008**, *47*, 2754–2787; *Angew. Chem.* **2008**, *120*, 2794–2828; b) J. W. Goodby, V. Görtz, S. J. Cowling, G. Mackenzie, P. Martin, D. Plusquellec, T. Benvegnu, P. Boullanger, D. Lafont, Y. Queneau, et al., *Chem. Soc. Rev.* **2007**, *36*, 1971–2032.

[2] *Handbook of Liquid Crystals* (Eds.: D. Demus, J. Goodby, G. W. Gray, H.-W. Spiess, V. Vill), Wiley-VCH, Weinheim, **1998**.

[3] a) X. Li, D. W. Bruce, J. M. Shreeve, *J. Mater. Chem.* **2009**, *19*, 8232–8238; b) C. Cruz, J. L. Galliani, B. Heinrich, D. W. Bruce, D. Guillon, *Mol. Cryst. Liq. Cryst.* **1999**, *330*, 1395–1402; c) C. Cruz, B.

Heinrich, A. C. Ribeiro, D. W. Bruce, D. Guillon, *Liq. Cryst.* **2000**, *27*, 1625–1631.
[4] K. Binnemans, *Chem. Rev.* **2005**, *105*, 4148–4204.
[5] a) J. Dupont, R. F. de Souza, P. A. Z. Suarez, *Chem. Rev.* **2002**, *102*, 3667–3691; b) T. Welton, *Chem. Rev.* **2004**, *248*, 2459–2477.
[6] C. K. Lee, H. W. Huang, I. J. B. Lin, *Chem. Commun.* **2000**, 1911–1912.
[7] a) A. E. Visser, R. P. Swatloski, S. T. Griffin, D. H. Hartman, R. D. Rogers, *Sep. Sci. Technol.* **2001**, *36*, 785–804; b) A. E. Visser, R. P. Swatloski, W. M. Reichert, R. Mayton, S. Sheff, A. Wierzbicki, J. H. Davis, R. D. Rogers, *Chem. Commun.* **2001**, 135–136; c) J. G. Huddleston, H. D. Willauer, R. P. Swatloski, A. E. Visser, R. D. Rogers, *Chem. Commun.* **1998**, 1765–1766.
[8] a) M. J. Grätzel, *Photochem. Photobiol. C* **2003**, 4, 145–153; b) N. Papageorgiou, Y. Athanassov, M. Armand, P. Bonhôte, H. Pettersson, A. Azam, M. J. Grätzel, *J. Electrochem. Soc.* **1996**, *143*, 3099–3108.
[9] a) N. Yamanaka, R. Kawano, W. Kubo, N. Masaki, T. Kitamura, Y. Wada, M. Watanabe, S. Yanagida, *J. Phys. Chem. B* **2007**, *111*, 4763–4769; b) S. Yazaki, M. Funahashi, J. Kagimoto, H. Ohno, T. Kato, *J. Am. Chem. Soc.* **2010**, *132*, 7702–7708.
[10] a) C. J. Bowlas, D. W. Bruce, K. R. Seddon, *Chem. Commun.* **1996**, 1625–1626; b) W. Dobbs, L. Douce, L. Allouche, A. Louati, F. Malbose, R. Welter, *New J. Chem.* **2006**, *30*, 528–532; c) K. M. Lee, Y. T. Lee, I. J. B. Lin, *J. Mater. Chem.* **2003**, *13*, 1079–1084; d) T. Mukai, M. Yoshio, T. Kato, H. Ohno, *Chem. Lett.* **2004**, *33*, 1630–1631; e) H. Yoshizawa, T. Mihara, N. Koide, *Mol. Cryst. Liq. Cryst.* **2004**, *423*, 61–72; f) J. Motoyanagi, T. Fukushima, T. Aida, *Chem. Commun.* **2005**, 101–103.
[11] a) A. Taubert, *Angew. Chem. Int. Ed.* **2004**, *43*, 5380–5382; *Angew. Chem.* **2004**, *116*, 5494–5496; b) W. Dobbs, J.-M. Suisse, L. Douce, R. Welter, *Angew. Chem. Int. Ed.* **2006**, *45*, 4179–4182; *Angew. Chem.* **2006**, *118*, 4285–4288; c) J.-M. Suisse, L. Douce, S. Bellemin-Laponnaz, A. Maisse-François, R. Welter, Y. Miyake, Y. Shimizu, *Eur. J. Inorg. Chem.* **2007**, 3899–3905; d) M. Yoshio, T. Ichikawa, H. Shimura, T. Kagata, A. Hamasaki, T. Mukai, H. Ohno, T. Kato, *Bull. Chem. Soc. Jpn.* **2007**, *80*, 1836–1841.
[12] X. Cheng, X. Bai, S. Jing, H. Ebert, M. Prehm, C. Tschierske, *Chem. Eur. J.* **2010**, *16*, 4588–4601.
[13] S. Yazaki, Y. Kamikawa, M. Yoshio, A. Hamasaki, T. Mukai, H. Ohno, T. Kato, *Chem. Lett.* **2008**, *37*, 538–539.
[14] a) H. Tokuhisa, M. Era, T. Tsutsui, *Appl. Phys. Lett.* **1998**, *72*, 2639–2641; b) Z. Peng, J. Zhang, *Chem. Mater.* **1999**, *11*, 1138–1143.
[15] X. Zhang, S. A. Jenekhe, *Macromolecules* **2000**, *33*, 2069–2082.
[16] M. M. Alam, S. A. Jenekhe, *Chem. Mater.* **2002**, *14*, 4775–4780.
[17] a) S. Torgova, L. Karamysheva, A. Strigazzi, *Braz. J. Phys.* **2002**, *32*, 593–601; b) M. Parra, P. Hidalgo, J. Alderete, *Liq. Cryst.* **2005**, *32*, 449–455; c) M. Parra, P. Hidalgo, E. Carrasco, J. Barbera, L. Silvino, *Liq. Cryst.* **2006**, *33*, 875–882.
[18] a) F. Lo Celso, I. Pibiri, A. Triolo, R. Triolo, A. Pace, S. Buscemi, N. Vivona, *J. Mater. Chem.* **2007**, *17*, 1201–1208; b) C. Rocaboy, F. Hampel, J. A. Gladysz, *J. Org. Chem.* **2002**, *67*, 6863–6870; c) X. Li, D. W. Bruce, J. M. Shreeve, *J. Mater. Chem.* **2009**, *19*, 8232–8238; d) I. Pibiri, A. Pace, S. Buscemi, V. Causin, F. Rastrelli, G. Saielli, *Phys. Chem. Chem. Phys.* **2012**, *14*, 14306–14314.
[19] a) B. S. Pedersen, S. Scheibye, K. Clausen, S. O. Lawesson, *Bull. Soc. Chim. Belg.* **1978**, *87*, 293–297; b) M. Kuroboshi, T. Hiyama, *Synlett* **1994**, 251–252; c) H. Gallardo, G. Conte, P. A. Tuzimoto, B. Behramand, F. Molin, J. Eccher, I. H. Bechtold, *Liq. Cryst.* **2012**, *39*, 1099–1111.
[20] a) J. Tao, J. Zhong, P. Liu, S. Daniels, Z. Zeng, *J. Fluorine Chem.* **2012**, *144*, 73–75; b) H. Chen, P. Liu, H. Li, S. Daniel, Z. Zeng, *Tetrahedron* **2013**, *69*, 5129–5135; c) H. Chen, P. Liu, H. Li, H. Zhang, S. Daniel, Z. Zeng, *Eur. J. Org. Chem.* **2013**, 7517–7527.
[21] a) A. R. Muci, S. L. Buchwald, *Top. Curr. Chem.* **2002**, *219*, 131–209; b) S. V. Ley, A. W. Thomas, *Angew. Chem. Int. Ed.* **2003**, *42*, 5400–5449; *Angew. Chem.* **2003**, *115*, 5558–5607; c) J. F. Hartwig, *Synlett* **2006**, 1283–1294; d) J.-P. Corbet, G. Mignani, *Chem. Rev.* **2006**, *106*, 2651–2710.
[22] Y. Wang, Z. Wu, L. Wang, Z. Li, X. Zhou, *Chem. Eur. J.* **2009**, *15*, 8971–8974.
[23] L. Zhu, G. Li, L. Luo, P. Guo, J. Lan, J. You, *J. Org. Chem.* **2009**, *74*, 2200–2202.
[24] A. E. Bradley, C. Hardacre, J. D. Holbrey, S. Johnston, S. E. J. McMath, M. Nieuwenhuyzen, *Chem. Mater.* **2002**, *14*, 629–635.
[25] Y. Matsunaga, T. Tsujimura, *Mol. Cryst. Liq. Cryst.* **1991**, *200*, 103–108.
[26] a) H. Debus, *Justus Liebigs Annalen der Chemie* **1858**, *107*, 199–208; b) Br. Radzisewski, *Ber. Dtsch. Chem. Ges.* **1882**, *15*, 2706–2708.
[27] a) W. R. Krigbaum, J. Watanabe, T. Ishilawa, *Macromolecules* **1983**, *16*, 1271–1279; b) A. D. Vries, *Mol. Cryst. Liq. Cryst.* **1973**, *24*, 337–345.
[28] a) K. Hoshino, M. Yoshio, T. Mukai, K. Kishimoto, H. Ohno, T. Kato, *J. Polym. Sci. Part A* **2003**, *41*, 3486–3492; b) D. Navarro-Rodriguez, Y. Frere, P. Gramain, D. Guillon, A. Skoulios, *Liq. Cryst.* **1991**, *9*, 321–335; c) L. Cui, V. Sapagovas, G. Lattermann, *Liq. Cryst.* **2002**, *29*, 1121–1132; d) H. Yoshizawa, T. Mihara, N. Koide, *Mol. Cryst. Liq. Cryst.* **2004**, *423*, 61–72; e) B. El Hamaoui, L. Zhi, W. Pisula, U. Kolb, J. Wu, K. Müllen, *Chem. Commun.* **2007**, 2384–2386.
[29] a) G. E. Logotheti, J. Ramos, I. G. Economou, *J. Phys. Chem. B* **2009**, *113*, 7211–7224; b) K. Dong, S. Zhang, D. Wang, X. Yao, *J. Phys. Chem. A* **2006**, *110*, 9775–9782; c) Y. Danten, M. I. Cabaco, M. Besnard, *J. Phys. Chem. A* **2009**, *113*, 2873–2889; d) R. Ozawa, S. Hayashi, S. Saha, A. Kobayashi, H. Hamaguchi, *Chem. Lett.* **2003**, *32*, 948–949.
[30] M. Shukla, N. Srivastava, S. Saha, *J. Mol. Struct.* **2010**, *975*, 349–356.
[31] H. Hamaguchi, R. Ozawa, *Adv. Chem. Phys.* **2005**, *131*, 85–104.
[32] E. R. Talaty, S. Raja, V. J. Storhaug, A. Dolle, W. R. Carper, *J. Phys. Chem. B* **2004**, *108*, 13177–13184.
[33] a) A. D. Becke, *Phys. Rev. A* **1988**, *38*, 3098–3100; b) C. Lee, W. Yang, R. G. Parr, *Phys. Rev. B* **1988**, *37*, 785–789.
[34] Gaussian 03, Revision D.01, M. J. Frisch, G. W. Trucks, H. B. Schlegel, G. E. Scuseria, M. A. Robb, J. R. Cheeseman, J. A. Montgomery Jr, T. Vreven, K. N. Kudin, J. C. Burant, J. M. Millam, S. S. Iyengar, J. Tomasi, V. Barone, B. Mennucci, M. Cossi, G. Scalmani, N. Rega, G. A. Petersson, H. Nakatsuji, M. Hada, M. Ehara, K. Toyota, R. Fukuda, J. Hasegawa, M. Ishida, T. Nakajima, Y. Honda, O. Kitao, H. Nakai, M. Klene, X. Li, J. E. Knox, H. P. Hratchian, J. B. Cross, V. Bakken, C. Adamo, J. Jaramillo, R. Gomperts, R. E. Stratmann, O. Yazyev, A. J. Austin, R. Cammi, C. Pomelli, J. W. Ochterski, P. Y. Ayala, K. Morokuma, G. A. Voth, P. Salvador, J. J. Dannenberg, V. G. Zakrzewski, S. Dapprich, A. D. Daniels, M. C. Strain, O. Farkas, D. K. Malick, A. D. Rabuck, K. Raghavachari, J. B. Foresman, J. V. Ortiz, Q. Cui, A. G. Baboul, S. Clifford, J. Cioslowski, B. B. Stefanov, G. Liu, A. Liashenko, P. Piskorz, I. Komaromi, R. L. Martin, D. J. Fox, T. Keith, M. A. Al-Laham, C. Y. Peng, A. Nanayakkara, M. Challacombe, P. M. W. Gill, B. Johnson, W. Chen, M. W. Wong, C. Gonzalez, J. A. Pople, Gaussian, Inc., Wallingford CT, **2004**.
[35] R. Dennington, T. Keith, J. Millam, K. Eppinnett, W. L. Hovell, R. Gilliland, **2003**, *GaussView*, version 3.09, Semichem, Inc., Shawnee Mission.
[36] X. Wang, C. S. Vogel, F. W. Heinemann, P. Wasserscheid, K. Meyer, *Cryst. Growth Des.* **2011**, *11*, 1974–1988.
[37] R. Lungwitz, V. Strehmel, S. Spange, *New J. Chem.* **2010**, *34*, 1135–1140.
[38] M. Hird, *Chem. Soc. Rev.* **2007**, *36*, 2070–2095.

Received: May 28, 2014
Published online: September 26, 2014